Response of Compliant Foils to Dynamic Loadings Produced by Oncoming Vortices

LCDR Mark M. Murray
Mechanical Engineering Department,
United States Naval Academy
Annapolis, MD 21402
410-293-6451
mmmurray@usna.edu

Laurens E. Howle
Department of Mechanical Engineering and Material Science
and Center for Nonlinear and Complex Systems,
Edmund T. Pratt, Jr. School of Engineering,
Duke University
Durham, NC 27708
919-660-5331
laurens.howle@duke.edu

Abstract

We investigate the change in induced drag generated by a lift producing control surface in an unsteady environment. When a lifting surface, such as a flap at an angle of attack, encounters disturbances in a fluid, the changing loads placed on the flap by the time-dependent flow cause the circulation about the flap to change. This changing circulation generates vorticity that sheds from the lifting surface. Accompanying the shed vorticity is an induced drag that is due solely to the time-dependent loading. The flexible region deforms in response to the time-changing fluid loading and modulates the circulation changes – hence, induced drag – that would otherwise occur with a rigid control surface. We use numerical simulation of inviscid flow coupled to a linear elastic control surface model to analyze induced drag reduction and the modification of lifting caused by surface flexibility. Arrays of oncoming free vortices of varying strength approximate the unsteady environment. Our results may aid in induced drag modification for specialized high-performance water craft.

Introduction

A body immersed in a fluid may be subjected to forces resulting from the relative motion between body and fluid. The forces exerted on the body are generally categorized as lift and drag, forces perpendicular and parallel, respectively, to the relative fluid motion. The drag forces are of several forms and vary in relative magnitude depending on the body geometry and flow type. Skin friction drag is the direct result of the shear stress induced on the body by a moving fluid of finite viscosity. The drag due to flow separation is another type of drag associated with viscosity. These two forms of drag are often lumped together and referred to as parasitic or profile drag (Kroo, 2001). A body producing lift is also subjected to losses associated with lift generation. These losses, often referred to as induced drag, arise from the momentum left in the fluid as a lifting body travels through it (Ashley & Landahl, 1965).

The various types of drag that are mentioned above are steady phenomena. Another form of drag is produced by a lift producing body in an unsteady environment. When a lifting surface encounters disturbances in the fluid, the changing loads placed on the body by the time-dependent flow cause the circulation about the body to change. This changing circulation generates vorticity that sheds from the lifting surface. Accompanying the shed vorticity is an induced drag that is due solely to the time-dependent loading (Katz & Plotkin, 2001).

A number of authors have investigated the physics of vortex-body interactions and the induced loading caused by this interaction (Rockwell 1998; So et al., 1999). There has also been work to suggest that vortex-body interactions can be utilized to efficiently propel an oscillating foil through a vortex array field (Streitlien et al., 1996) and to reduce the overall drag forces in a fishlike model (Barrett et al., 1999). Much of the work in this area is primarily inspired by examples given in nature (Azuma, 1992).

Nature also provides examples of increased efficiency through passive drag reductions by means of compliant structures (Pabst et al., 1999). Our method of passive drag modification uses a control surface with a flexible trailing region. The flexible region deforms in response to the time-changing fluid loading and modulates the circulation changes – hence, induced drag – that would otherwise occur with a rigid control surface. We use numerical simulation of inviscid flow coupled to a linear elastic control surface model to analyze induced drag reduction and the modification of lifting caused by surface flexibility. Arrays of oncoming vortices of varying strength approximate the unsteady environment. The goal of this work is to demonstrate that the unsteady drag force on a lift producing foil can be changed by allowing compliancy in the trailing three quarter chord of the foil.

Mathematical Model Development

To obtain insight into the dynamics of unsteady drag production we choose a simplified two-dimensional model that includes the pertinent physical aspects. We choose not to include steady drag effects, so as to more clearly analyze the effects of the unsteady drag. We utilize a linear elastic beam equation to model our structure, and a vortex lattice method to simulate the hydrodynamic portion. The structural and hydrodynamic portions of the model are directly coupled. Arrays of convecting vortices approximate the unsteady disturbances in the fluid.

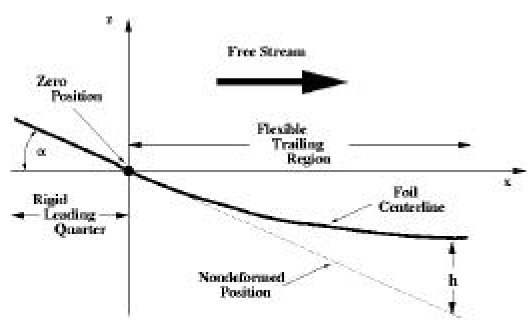

Figure 1: Diagram of Coordinates for Foil

Figure 1 shows the general coordinate diagram utilized for the structural and hydrodynamic equations. For our model we assume that the leading edge quarter chord has infinite stiffness and does not deform. The region of the foil trailing the quarter chord point is compliant and deforms in response to the steady and unsteady hydrodynamic forces placed on it. The following sections show a more detailed explanation of the model setup and the equations utilized to describe the model.

Structural Equation

The flexible control surface is assumed to be a two-dimensional plate. This 2-D plate is assumed to have sufficiently small deflections and behaves in a linear elastic manner. The angle of attack remains sufficiently small so that the beam deflection is assumed to be in the z-direction only. The unsteady equation that describes the structure is

$$r_S''(x)\frac{\partial^2 h(x,t)}{\partial t^2} + \frac{\partial^2}{\partial x^2}\left(EI(x)\frac{\partial^2 h(x,t)}{\partial x^2}\right) = \Delta p(x,t) \qquad (1)$$

where $r_S''(x)$ is the mass per unit chord length, $h(x,t)$ is the vertical displacement of the beam from its nondeformed position, E is the modulus of elasticity, $I(x)$ is the moment of inertia per unit span, and $\Delta p(x,t)$ is the difference in pressure between the top and bottom of the foil. It is noted that the moment of inertia is allowed to vary along the chord of the foil. For all examples of this work we assume a NACA 0012 airfoil cross-section to calculate thickness values for the structural model (Ladson, 1996).

Hydrodynamic Equations

We assume that the fluid field is incompressible, inviscid, and irrotational. The fluid field can therefore be described using the potential flow model. The equation that describes the field is

$$\nabla^2\Phi = 0 \qquad (2)$$

where Φ is the velocity potential. The relationship between the velocity potential and pressure can be derived from the momentum equation. Assuming small disturbances and linear theory, the pressure difference between the upper and lower surfaces of the foil is

$$\Delta p(x,t) = r\left(U_\infty \frac{\partial}{\partial x}\Delta\Phi + \frac{\partial}{\partial t}\Delta\Phi\right) \qquad (3)$$

Where r is the fluid density, U_∞ is the mean free stream velocity, and $\nabla\Phi$ is the velocity potential difference between the and bottom of the foil.

An unsteady discrete vortex lattice model is used to describe the hydrodynamic portion of the problem. In this discrete model the pressure difference of equation (3) at a time t becomes

$$(\Delta p)_j = \frac{rU_\infty}{\Delta x}\Gamma_j + r\frac{\partial}{\partial t}\sum_{i=1}^{j}\Gamma_i \qquad (4)$$

where Γ is the discrete vortex strength.

The unsteady nature of the problem is introduced to the otherwise non-time dependent hydrodynamic equation through the unsteady boundary conditions. This manifests itself in the vortex lattice model through the equations that describe the induced and prescribed downwash at each panel. This equation is

$$U_\infty\left(a - \left.\frac{\partial h}{\partial x}\right|_i\right) - \left.\frac{\partial h}{\partial t}\right|_i = \sum_{j=1}^{N_F}\Gamma_j\frac{z_j - z_i}{2pr_j^2} + \sum_{k=1}^{N_W}\Gamma_{Wk}\frac{z_k - z_i}{2pr_k^2} + \sum_{l=1}^{N_D}\Gamma_{Dl}\frac{z_l - z_i}{2pr_l^2} \qquad (5)$$

where a is the nondeformed angle of attack and h is the vertical deflection of the beam from its nondeformed position. The three summations on the right hand side of equation (5) account for the induced wash due to the bound vorticity of the foil, the vorticity shed into the wake, and the disturbance vorticity, respectively.

The drag on the foil due to unsteady loads is calculated using the equation suggested by Katz and Plotkin (2001) for a lumped vortex model. The drag equation utilized is

$$D = \sum_{j=1}^{N} r \left(w_{W_j} \Gamma_j + \frac{\partial}{\partial t} \sum_{k=1}^{j} \Gamma_k \Delta x \sin a_k \right) \quad (6)$$

where N is the number of panels used to model the foil, w_W is the wash induced by the wake at the three quarter chord point, Δx is the individual panel length, and a_k is the local angle of attack of each panel.

The convection of the individual vortices is described by

$$x_i^{n+1} = x_i^n + \left(U_\infty + u_i^n \right) \Delta t \quad (7)$$

and

$$h_i^{n+1} = h_i^n + w_i^n \Delta t \quad (8)$$

where x_i^{n+1} and h_i^{n+1} are the calculated x and z positions of an individual vortex at the new time, Δt is the time step, and U_∞ is the free stream velocity. The terms u_i^n and w_i^n are the x and z induced velocities. For the case of a fixed wake or a fixed vortex disturbance array, the induced velocities, u_i^n and w_i^n, are assumed to be zero. When the influence of the vortices in the free stream is considered, the induced velocities become

$$\begin{aligned} u_i^n = &\sum_{j=1}^{N_F} \frac{-\Gamma_j^n \left(h_j^n - h_i^n \right)}{\left(x_j^n - x_i^n \right)^2 + \left(h_j^n - h_i^n \right)^2 + e} \\ &+ \sum_{j=1}^{N_W} \frac{-\Gamma_{W_j}^n \left(h_j^n - h_i^n \right)}{\left(x_j^n - x_i^n \right)^2 + \left(h_j^n - h_i^n \right)^2 + e} \\ &+ \sum_{j=1}^{N_D} \frac{-\Gamma_{D_j}^n \left(h_j^n - h_i^n \right)}{\left(x_j^n - x_i^n \right)^2 + \left(h_j^n - h_i^n \right)^2 + e} \end{aligned} \quad (9)$$

and

$$\begin{aligned} w_i^n = &\sum_{j=1}^{N_F} \frac{-\Gamma_j^n \left(x_j^n - x_i^n \right)}{\left(x_j^n - x_i^n \right)^2 + \left(h_j^n - h_i^n \right)^2 + e} \\ &+ \sum_{j=1}^{N_W} \frac{-\Gamma_{W_j}^n \left(x_j^n - x_i^n \right)}{\left(x_j^n - x_i^n \right)^2 + \left(h_j^n - h_i^n \right)^2 + e} \\ &+ \sum_{j=1}^{N_D} \frac{-\Gamma_{D_j}^n \left(x_j^n - x_i^n \right)}{\left(x_j^n - x_i^n \right)^2 + \left(h_j^n - h_i^n \right)^2 + e} \end{aligned} \quad (10)$$

where the e is introduced to prevent the 'encounter problem' (Krasney, 1987; Hall & Hall, 2000). The three summations account for the induced velocity due to the bound vorticity of the foil, the vorticity shed into the wake, and the disturbance vorticity respectively.

Terminology for Results

The parameter that distinguishes the different compliant foils is the bending stiffness of the two-dimensional plate. For our purposes we define the bending stiffness as the dimensionless parameter given by

$$K_B = \frac{Ed^3/12}{1/2\, rU_\infty^2 c^3} \quad (11)$$

where E is the modulus of elasticity, d is the foil thickness at the quarter chord, r is the fluid density, U_∞ is the mean free stream velocity, and c is the chord length.

The lifting and drag forces are normalized in the standard manner as the coefficient of lift (C_L) and drag coefficient (C_D). The coefficient of lift and drag coefficient in two dimensions are

$$C_L = \frac{L'}{1/2\, rU_\infty^2 c} \quad (12)$$

and

$$C_D = \frac{D'}{1/2\, rU_\infty^2 c} \quad (13)$$

Where L' and D' are the lift and drag forces per unit span respectively. To more explicitly demonstrate the effect of bending stiffness, the diagrams in this work present the drag as a ratio of drag coefficients. The drag ratio (*DR)* is

$$DR = \frac{C_D}{C_{D,K_B=\infty}} \quad (14)$$

where $C_{D,K_B=\infty}$ is the time averaged unsteady drag coefficient for a foil with infinite bending stiffness.

Equilibrium Angle of Attack

To accurately compare the drag and lifting forces on foils of differing bending stiffness, the angle of attack of the leading quarter chord is varied to ensure the equality of the steady state lift of the contrasted foils. Because of the response of a compliant structures, leading quarter chord angle of attack of foils with smaller bending stiffness will be greater than those of larger bending stiffness because of the decreased ability of the compliant trailing region to support a hydrodynamic load.

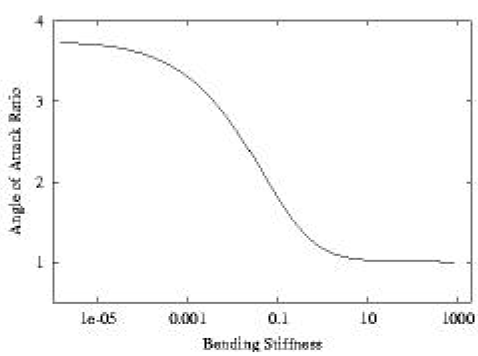

Figure 2: Bending Stiffness vs. Angle of Attack Ratio for NACA 0012 Foil Shape

Figure 2 shows the leading edge angle of attack ratio (ratio of leading edge angle of attack of a finite stiffness foil to a foil of infinite stiffness) plotted against bending stiffness. Figure 2 shows that for small bending stiffness the angle of attack ratio approaches a value of 4.0, which is to be expected when the load carrying capability of the trailing three quarter chord goes to zero. At this point all of the hydrodynamic load is carried by the leading edge quarter chord.

The plot gives the authors a reasonable range of stiffness values to investigate. The limits of this range are determined by ensuring the proper matching of the hydrodynamic force and impedance of structural response.

Single Disturbance

The most basic test of the effects on lift and drag that disturbances have on a foil is the interaction of a single disturbance. The vortex disturbance starts upstream of the foil with an initial horizontal displacement and convects downstream. The individual vortex strength is presented as a factor of the foil's steady state circulation value. For all cases of this work we will present the strength of the individual vortices as a multiple of the foil's steady state circulation.

We choose to present only one specific single disturbance case to illustrate the effect that bending stiffness has on the drag exerted on the foil in the single disturbance model. The diagram shown in Figure 3 presents the results for the specific chosen case. Figure 3 is a plot of bending stiffness to drag ratio for a NACA 0012 foil at a five degree angle of attack that interacts with a single vortex disturbance. The vortex strength is one half of the foil steady state circulation. The vortex is released 30 chord lengths upstream and one chord length below the foil zero position. The disturbance vortex and vortices shed from the foil are convected with the free stream and induced velocities of the free wake model.

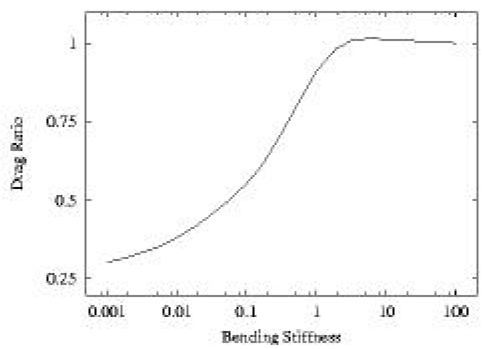

Figure 3: Bending Stiffness vs Drag Ratio for Single Vortex Disturbance

Figure 3 demonstrates that significant differences in unsteady drag force are achievable for foils carrying the same steady lifting force and differing only in bending stiffness. This particular case shows that as the bending stiffness is decreased from infinity the unsteady drag magnitude increases slightly and then begins to decrease dramatically for bending stiffness values less than 1.0.

Multiple Disturbances – Vortex Arrays

There is a possibility of exciting a resonant phenomenon that may alter the unsteady drag and lifting forces of a foil of finite bending stiffness (So et al.,1999). This phenomenon is explored by allowing arrays of vortices that are convecting with the free stream to interact with a compliant foil. Two types of multiple disturbance arrays are briefly explored in this work. The first places the foil in between the two arrays of vortices in a vortex street. This geometry is similar to the geometry utilized by So and Mignolet (1999) and Gopalkrishnan et al. (1994) in their studies of vortex-foil interactions. The second geometry offsets the foil from a single array of vortices of alternating strength values.

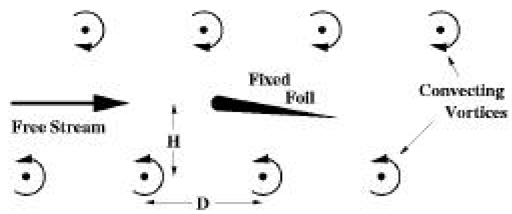

Figure 4: Diagram of Dual Rows of Vortices

Figure 4 shows a basic diagram of a foil at the center of a Karman vortex street. The distance between vortices is D and the distance between the two vortex arrays is $2H$ (with the foil zero point centered between the two arrays). Both of these values are normally presented as factors of chord. All individual vortices have the same strength, which is presented as a multiple of the steady state foil circulation.

Once again we choose to present the results for a specific case of this type of vortex interaction. Figure 5 is a plot of the bending stiffness vs. drag ratio for a NACA 0012 foil at a five degree angle of attack at the center of a Karman vortex street. The individual vortex strengths are equal to the value of circulation of the foil at steady state, the half distance between the arrays (H) is equal to one chord length, and the distance between vortices (D) is equal to two chord lengths. For this case the fixed wake model is utilized where the disturbance vortices and the vortices shed from the foil are convected with the free stream velocity only.

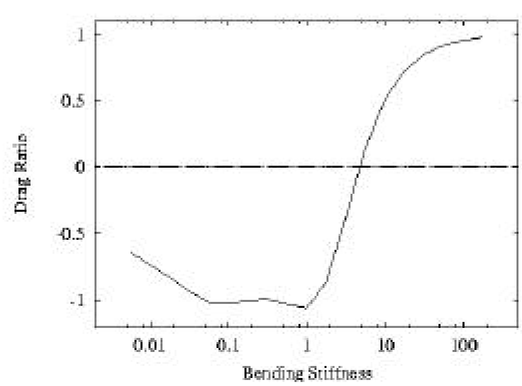

Figure 5: Bending Stiffness vs. Drag Ratio for Dual Vortex Rows

Figure 5 shows the difference in unsteady drag that is obtained for different bending stiffness values. The case presented shows a variation of over 200% in unsteady drag. Once again demonstrating the significant differences in unsteady drag that are achievable by varying the stiffness of the foil. There is also weakly defined relative extrema that occur for bending stiffness of 0.1 and 1.0. These extrema correspond to the well defined extremum shown in Figure 7.

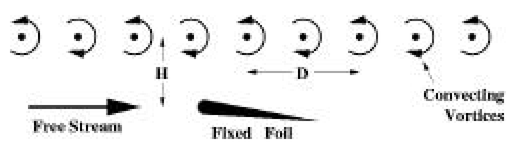

Figure 6: Single Row of Alternating Convecting Vortices

Figure 6 shows a basic diagram of the geometry the second type of multiple disturbance array. In this geometry the foil is offset below a single array of equally spaced vortices, that are of equal magnitude strength, but alternate in direction of rotation. The distance between the foil zero point and the array is H, the offset distance. The distance between vortices of similar rotation is D.
The results of the specific case we choose to present are shown in Figure 7. Figure 7 is a plot of bending stiffness vs. drag ratio for a NACA 0012 foil at a five degree angle of attack offset from a single array of alternating vortices. The individual vortex strengths are equal to the value of circulation of the foil at steady state, the offset distance (H) is one chord length, the distance between similar vortices (D) is two chord lengths. For this case the fixed wake model is utilized. Therefore the induced velocities are zero and the disturbance and shed vortices are convected with the free stream velocity only.

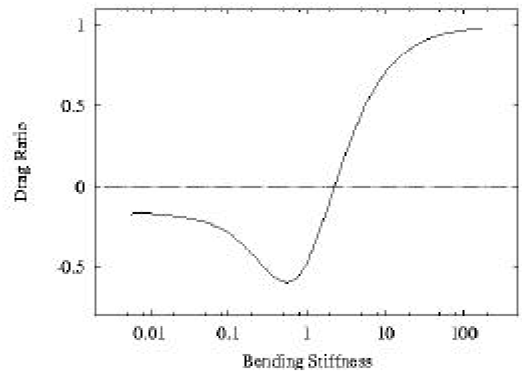

Figure 7: Bending Stiffness vs. Drag Ratio for Single Row Alternating Vortices

Figure 7 once again demonstrates the significant change in unsteady drag that is achievable. The figure also shows a clearly defined local extremum appearing at a bending stiffness of 0.6. The appearance of this clearly defined extremum suggests that a structural resonance phenomena is occurring.

Conclusions

The goal of this work is to demonstrate that the unsteady drag force can be altered by changing the bending stiffness of the trailing three quarter chord of a compliant foil. The three types of vortex disturbance analyzed in this work to demonstrate the change in unsteady drag force are a single vortex disturbance, dual vortex arrays, and a single alternating strength vortex array. The results of the three specific cases that are presented all demonstrate that varying the bending stiffness of the foil will significantly alter the unsteady drag forces that are felt by foils supporting the same steady lifting force. Not presented in this paper is the dramatic effect that compliancy has on the lifting force perturbations caused by the perturbations.

There are several areas of future work planned for this topic. The first is to analyze more closely the areas of structural and hydrodynamic resonance as they relate to both the unsteady drag and lifting forces. We also intend to construct a test apparatus to confirm the numerical results presented in this work. The results of this and future work may aid in the induced drag reduction for specialized high-performance water craft and for vehicles that utilize compliant foils for propulsion (Hobson et al., 1999).

Acknowledgements

This work is supported by the Office of Naval Research through grant N00014-99-1-0452.

Bibliography

Ashley, H. & Landahl, M. 1965. *Aerodynamics of Wings and Bodies*, Dover.

Azuma, A. 1992. *The Biokinetics of Swimming and Flying*, Springer-Verlag.

Barrett, D.S., Triantafyllou, M.S., Yue, D.K.P., Grosenbaugh, M.A. & Wolfgang, M.J., 1999. "Drag reduction in fish-like locomotion", *Journal of Fluid Mechanics* **392**:183-212.

Gopalkrishnan, R., Triantafyllou, M.S., Triantafyllou, G.S. & Barrett, D. 1994. "Active vorticity control in a shear flow using a flapping foil", *Journal of Fluid Mechanics* **274**:1-21.

Hall, K.C. & Hall, S.R. 2000. "A rational engineering analysis of the efficiency of flapping flight", Presented at the Conference on Fixed, Flapping, and Rotary Wing Vehicles at Very Low Reynolds Numbers, Notre Dame, IN, June 5-7.

Hobson, B., Pell, C. & Murray, M.M. 1999. "Pilotfish: Maximizing agility in an unmanned-underwater vehicle", *Proc. 11^th^ Int. Symp. Unmanned Untethered Submersible Tech.*, Durham, NH, 23-25 Aug 1999, 41-51.

Katz, J. & Plotkin A. 2001. *Low Speed Aerodynamics*, Cambridge University Press, 2^nd^ Edition.

Krasney, R. 1987. "Computation of vortex sheet roll-up in the Trefftz plane", *Journal of Fluid Mechanics* **184**:123-155.

Kroo, I. 2001. "Drag due to lift: Concepts for prediction and reduction", *Annual Review of Fluid Mechanics* **33**:587-617.

Ladson, C.L., Brooks, C.W., Hill, A.S. & Sproles, D.W. 1996. "Computer program to obtain ordinates for NACA airfoils", *NASA Technical Memorandum 4741*, December 1999.

Pabst, D.A., Hamilton, J.L., McLellan, W.A., Williams, T.M. & Gosline, J.M.1999. "Streamlining Dolphins: Designing soft-tissue keels", *Proc. 11^th^ Int. Symp. Unmanned Untethered Submersible Tech.*, Durham, NH, 23-25 Aug 1999, 477-486.

Rockwell, D. 1998. "Vortex-body interactions", *Annual Review of Fluid Mechanics* **30**:199-229.

So, R.M.C., Jadic, I. & Mignolet, M.P. 1999. "Fluid-structure resonance produced by oncoming alternating vortices", *Journal of Fluids and Structures* **13**:519-548.

Streitlien, K., Triantafyllou, G.S. & Triantafyllou, M.S. 1996. "Efficient foil propulsion through vortex control”, *AIAA Journal* **34**: No. 11, 2315-2319.